The Meteoritical Society

Meteoritics & Planetary Science 50, Nr 12, 2045–2066 (2015)
doi: 10.1111/maps.12566

Glass-bearing inclusions in Shergotty and Chassigny: Consistent samples of a primary trapped melt?

Maria Eugenia VARELA[1*] and Ernst ZINNER[2]

[1]Instituto de Ciencias Astronómicas de la Tierra y del Espacio (ICATE), Av. España 1512 sur, San Juan, Argentina
[2]Laboratory for Space Sciences and the Physics Department, Washington University, St. Louis, Missouri 63130, USA
[*]Corresponding author. E-mail: evarela@icate-conicet.gob.ar

(Received 23 September 2014; revision accepted 15 September 2015)

Note for Ernst Zinner

Dr. Ernst K. Zinner died Thursday, 30 July 2015, at the age of 78 of complications of mantle cell lymphoma. I wish to express my deepest thanks to Ernst for his invaluable help and generosity during all these years, for his stimulating talks, but mainly for giving me the privilege of his friendship.

Abstract–Glass-bearing inclusions hosted by different mineral phases in SNC meteorites provide important information on the conditions that prevailed during formation of early phases and/or on the composition of the primary trapped liquids/melts of these rocks. Although extensive previous work has been reported on such inclusions, several questions are still unresolved. We performed a chemical and petrographic study of the constituents (glasses and mineral assemblage) of glassy and multiphase inclusions in Shergotty and Chassigny. We focused on obtaining accurate trace element contents of glasses and co-existing minerals and discussing their highly variable REE contents. Our results reveal an unusual geochemistry of trace element contents that appear to be independent of their major element compositions. Chemical equilibrium between phases inside inclusions as well as between glasses and host minerals could not be established. The LREE contents of glasses in glass inclusions can vary by up to two orders of magnitude. The depletion in trace element abundances shown by glasses seem to be inconsistent with these phases being residual melts. The light lithophile element contents of glasses are highly variable with enrichment in incompatible elements (e.g., Be, Sr, Ba, and LREE) indicating some processes involving percolation of fluids. All of these features are incompatible with glass-bearing inclusions in the host minerals acting as closed systems preserving unmodified primary liquids/melts. Glass-bearing inclusions in Shergotty and Chassigny appear to have been altered (as was the rock itself) by different postformational processes (e.g., shock, metamorphism, metasomatic [?] fluids) that affected these meteorites with different degree of intensity. Our results indicate that these inclusions could not preserve a reliable sample of the primary trapped melt.

INTRODUCTION

The Shergotty and Chassigny achondrites are members of the oblivious SNC (Shergotty-Nakhla-Chassigny) meteorites, which are believed to have originated from Mars (e.g., McSween 1994). Of all SNC meteorites recognized up to date, shergottites are the most abundant group. They are commonly divided into three types: basaltic, lherzolitic, and olivine-phyric (Goodrich 2002).

The Shergotty meteorite belongs to the basaltic type. It is a cumulate rock, consisting of oriented pyroxene crystals with interstitial maskelynite and minor (~2%) titanomagnetite and merrillite (e.g., Stolper and McSween 1979). Pyroxene crystals account for almost 70% of the rock and have homogeneous Mg-rich cores and strongly zoned rims (Stolper and McSween 1979; Wadhwa et al. 1994). Shergotty records a two-stage crystallization history; early co-crystallization of augite and pigeonite (at 56 MPa and

hydrous conditions), followed by crystallization of the intercumulus liquid at shallow depth under anhydrous conditions (e.g., Dann et al. 2001). Several studies on the distribution of light lithophile elements showed that the cores of the pyroxenes are enriched in Li and B compared to the rim (in which Be > Li and B) indicating degassing of water from magmas as pyroxenes are carried to shallow depths during ascent (e.g., Lentz et al. 2001; McSween et al. 2001; Beck et al. 2006). However, the gradual decrease in Li abundances from core to rim raises questions concerning the role of diffusional equilibration processes. Later results showed that the distributions of Li and B in the shergottite pyroxene from Shergotty and Zagami are consistent with subsolidus diffusional processes (e.g., Beck et al. 2006; Treiman et al. 2006; William et al. 2010), as reported by the study of Li distribution in augite grains from MIL 03346 (Richter et al. 2013). In Shergotty, like in other basaltic shergottites, glass-bearing inclusions are present not only in early crystallizing pyroxenes (augite and pigeonite), but in mineral phases (e.g., merrillite and titanomagnetite) throughout the entire crystallization sequence.

The Chassigny achondrite consists of Fe-rich olivine (Fo_{68}) with anhedral to euhedral shape, suggestive of a cumulate origin (e.g., Floran et al. 1978; Wadhwa and Crozaz 1995; McSween and Treiman 1998). The various studies performed to determine the chemical composition of the parent magma of different cumulate rocks (e.g., Chassigny and Nakhla) focused on the studies of glass-bearing inclusions and experimental crystallization studies. Although both approaches seem quite straightforward, they give very different results. On the one hand, the study of glass-bearing inclusions (e.g., Johnson et al. 1991; Harvey and McSween 1992; Treiman 1993) indicates that the parent magma of these rocks was Fe-rich and Al-poor. On the other hand, experimental studies performed on the proposed compositions were unable to produce the assemblage of phases observed in Chassigny, at low and at high pressures and under dry and hydrous conditions (Minitti and Rutherford 2000; Filiberto et al. 2005).

Glass-Bearing Inclusions in SNC Meteorites, A Brief Overview

Glass-bearing inclusions have been extensively studied in all of the SNC meteorites to deduce the composition of the melt from which these meteorites formed (e.g., Floran et al. 1978; Treiman 1986, 1993; Johnson et al. 1991; Harvey and McSween 1992; Varela et al. 2000, 2001; Goodrich 2003; Stockstill et al. 2005; Filiberto 2008; Peslier et al. 2010; Basu Sarbadhikari et al. 2011; Sautter et al. 2012; Goodrich et al. 2013). Although extensive work has been performed on such inclusions, several questions are still unanswered, as glass inclusions can be affected by significant postentrapment crystallization and/or re-equilibration with the host mineral that could modify their initial composition.

Glass-bearing inclusions represent small volumes of the co-existing melts/liquids trapped during growth of their host crystals. They are assumed to represent pristine samples of melts/liquids that formed in thermodynamic equilibrium with their host minerals. From their bulk chemical composition, that of the parent melt can be calculated by assuming that the mineral phases inside the multiphase inclusions (MIs) are daughter minerals formed during the cooling of the trapped melt. Their bulk chemical compositions after re-integration of daughter minerals and correction for re-equilibration with the host and wall crystallization are used to reconstruct the composition of the parent magma and the conditions of their formation (e.g., Roedder 1984).

To reconstruct the initial liquid composition, two methods can be applied. The first, and most frequently used, takes into account the modal abundances and average compositions of constituting phases to obtain the present bulk composition of the inclusions (e.g., Goodrich 2003; Peslier et al. 2010; Basu Sarbadhikari et al. 2011). This bulk composition needs addition of olivine or pyroxene so the calculated composition is at equilibrium with the host mineral, as crystallization of the host phase onto the inclusion's walls and Fe/Mg re-equilibration are common processes taking place during cooling (e.g., Sobolev 1996; Danyushevsky et al. 2002). Although, this method is based on reasonable assumptions, it leads to a simplification of this complex natural system. Reconstruct the trapped melt composition using numerical modeling is mainly used for olivine-hosted melt inclusions (e.g., Sobolev and Shimizu 1993a, 1993b; Danyushevsky et al. 2000; Gaetani and Watson 2000). These results are dependent on the extent of the melt inclusion/host mass exchange and involve an accurate knowledge of the oxidation state and volatile contents of the melt (Danyushevsky et al. 2002). However, these required parameters are not well constrained in several of the SNC meteorites.

In the second method, the whole inclusion (glass + crystals inside the inclusion + the layer of the host mineral crystallized onto the inclusion's walls) is treated in experiments that allow reversal of the processes that occurred inside the inclusions during cooling. While this method is least model dependent, it faces numerous experimental difficulties, most commonly decrepitation of the inclusions during heating (e.g., Varela et al. 2001; Stockstill et al. 2005; Sautter et al. 2012). Thus,

reconstruction of chemical composition of primary trapped liquid (PTL) using previously described methods gives different results and, therefore, it seems to be model dependent. Also, it may suggest that experimental rehomogenization has issues that need to be resolved and consequently is not such a reliable technique. This problem is more serious when visual control during homogenization experiments is not performed, as it is impossible to observe phase transformations within inclusions or to determine the appropriate duration/heating rate for the experiments (Danyushevsky et al. 2002). However, a recent study of glass inclusions in Nakhla (Goodrich et al. 2013) using analytical methods rather than experimental rehomogenization of glass inclusions could bridge the gap between both methods. Their estimate PTL in augite (Goodrich et al. 2013) turned out to be higher in SiO_2 and K_2O and lower in FeO as compared to single rehomogenized melt inclusions selected as the preferred Nakhla parent magma composition by Stockstill et al. (2005) and Sautter et al. (2012), but compositionally similar to that derived as the average composition of all (4) inclusions that were rehomogeneized by Varela et al. (2001). These results show that experimental rehomogenization, if based on nonselected data, can guarantee retrieval of the PTL.

Some Considerations Regarding the Heating Experiments on Primary Glass-Bearing Inclusions in SNC Meteorites

The first experimental heating tests of primary glass-bearing inclusions from Nakhla and Chassigny (Varela et al. 2000, 2001) revealed that these inclusions behave differently throughout comparable heating runs (Varela et al. 2003).

During heating experiments of primary glass-bearing inclusions in Nakhla, the glass was melted and the crystals inside the inclusions dissolved in the melt. They mimic a parental melt that has subsequently evolved as a closed system during cooling. However, the quenched homogenized glass turned out to be out of chemical equilibrium with the host augite (Varela et al. 2001). Although the duration of the experiments were enough to dissolve the crystalline phases inside inclusions, the lack of chemical equilibrium with the host augite could indicate that the duration was not enough for remelting the right amount of the host phase. However, by adding 5, 10, and 20 vol% of augite (core composition) to the experimentally determined melt composition, the calculated augite-melt Kd(Fe) for these liquids of 0.43, 0.46, and 0.52, respectively, are also out of equilibrium. In principle, and due to the dissolution of crystals inside inclusions in augites during heating, inclusions hosted by augites mimic at least in part parental melt inclusions (Varela et al. 2001).

Conversely, during heating experiments of primary glass-bearing inclusions of Chassigny (final temperature of 1200 °C) the crystalline phases within inclusions did not dissolve. This result could mean that our attempt to rehomogenize the Chassigny inclusions failed. However, the chemical composition of the quenched glass turned out to be in equilibrium with the host olivine (Varela et al. 2000). The quench glasses from the experimentally heated inclusions in Chassigny show increased orthoclase contents, suggesting inhomogeneity with respect to certain elements (e.g., K_2O, CaO) (Varela et al. 2000).

The question that arises is why similar primary glass-bearing inclusions exposed to similar experimental heating runs behave so differently?

The main distinction among them is that the primary inclusions in Chassigny are surrounded by open radial cracks which are scarce or nonexistent in glass inclusions in augite from Nakhla. Could these radial cracks serve as paths that allow part of the melt to flow away from the inclusion, or make the inclusions vulnerable to remobilization of some species during postentrapment (late metasomatic) processes thus, contributing to alter an otherwise ideal closed-system? If so, then these inclusions might not be able to retain a pristine composition and their effectiveness at preserving unmodified primary trapped liquids/melts can be called into question.

To find an answer to these issues, we performed a detailed chemical (major and trace element) study of the different constituent phases of glassy and multiphase inclusions (GIs and MIs) in Chassigny and Shergotty. Both meteorites are characterized by having their GIs and MIs surrounded by radial cracks.

SAMPLES AND ANALYTICAL TECHNIQUES

The Shergotty polished thin sections (PTS) A and B and the Chassigny PTS L6101 (NHM, Vienna) were studied by microscopic and microanalytical techniques. Scanning electron microscopy was performed with a Jeol 6400 (NHM, Vienna) with a sample current of 1 nA and an acceleration voltage of 15 kV. Mineral major element compositions were measured with a SX100 CAMECA electron microprobe (University of Vienna). To reduce loss of Na from glasses during analysis, this element was analyzed first with a counting time of 5 s and a defocused beam (5 μm). For Cl measurements, the counting times were increased to 20 s. Under these operating conditions, the error on Cl measurements is 10%. The accuracy for the analyzed elements was established by replicate analyses of

basaltic and rhyolitic standard glasses (CFA, ALV 981, VNM50, and KE12; Mosbah et al. 1991).

Trace element analyses of minerals and glasses were made with a Cameca IMS 3F ion microprobe at Washington University (St. Louis) following a modified procedure of Zinner and Crozaz (1986). Samples were bombarded with an O^- primary beam of either 14.5 or 17 keV energy focused into a spot 5–25 μm in diameter. The beam currents range from 3 to 20 nA and positive secondary ions were accelerated through a voltage of 4500 V. Considering the small size of the grains to be analyzed inside inclusions a field aperture close to the image plane of the sample surface was inserted into the ion beam, allowing only ions from a restricted area (<10 μm diameter) to be accepted. Measurements were performed by cycling (between 10 and 30) through a series of mass peaks in an automatic peak jumping mode. Contamination by hitting some phases at depth was controlled by checking the element signal with depth. Thereby, in three inclusions (2 GIs and 1 MI) trapped by merrillite, we could detect contamination by the host phase after the first five cycles, as the element signals were highly variable.

RESULTS

Petrography of the Rocks

In the Shergotty samples, pyroxenes are usually lath-shaped to subhedral with a medium grain size of ~1 mm. Titanomagnetite and merrillite occur as euhedral to subhedral interstitial grains. Merrillite forms mainly elongate and straight crystals, but few show a curved shape. This shape becomes evident due to the presence of thin curved titanomagnetite that partially decorates the crystal surface.

The Chassigny achondrite consists of Fe-rich olivine (Fo_{68}) with undulatory extinction, abundant irregular fractures, and glass-bearing inclusions; it also has minor low-Ca pyroxene and chromite grains. Most olivine crystals are anhedral, with few of them being subhedral. The minerals in the thin section have a medium grain size of 1–1.5 mm and an equigranular texture.

Petrography of Glass Inclusions

Shergotty sections A and B contain two types of glass inclusions: GIs and MIs (Figs. 1A–D). The latter consist of glass and <60 μm crystals of low–Ca pyroxene (Px), high-Ca pyroxene (Cpx), kaersutite, apatite, spinel, and iron sulfide (FeS). Kaersutite-bearing inclusions are mainly observed in pigeonite, but one has also been observed in augite (Varela and Zinner 2013).

Glass-bearing inclusions trapped by augite and pigeonite have irregular shapes (Fig. 1A). Both types of inclusions (GIs and MIs) occur in the core or in the rim of pyroxene crystals with sizes ranging from 10 to 50 μm for GIs and 30 to 120 μm for MIs. Both types of inclusions can coexist within a single pyroxene grain.

Glass-bearing inclusions trapped by merrillite and titanomagnetite are usually round or ellipsoidal (Figs. 1B–D). In merrillite, GIs (~10 μm in size) are mainly aligned at the center of elongate crystals while MIs (~30–50 μm in size) are often observed to occur in isolation. Several of the MIs hosted by merrillite have a rim composed of euhedral and subhedral crystals of titanomagnetite (TiO_2: 22–23 wt%, FeO: 71–72.6 wt%, Al_2O_3: ~2.5 wt%), low-Ca pyroxene, and few sulfides (Fig. 1D).

Three types of glass-bearing inclusions are present in Chassigny olivines: pure glass (glassy), monocrystal (glass plus a single mineral phase), and multiphase (glass plus several mineral phases) inclusions that have been described in detail by Varela et al. (2000), therefore only a brief description is provided here.

Multiphase inclusions have variable sizes (>20 μm, up to 150 μm in apparent diameter), with a subrounded or euhedral (negative crystal) shape. Crystals in all MIs in Chassigny are rich in fractures while the coexisting glass is free of them. The studied multiphase inclusion (Fig. 1E) has a subrounded elongated shape, with a major axis of 150 μm and occurs isolated in the host olivine. Among the several MIs present in Chassigny this inclusion was particularly interesting for two main reasons. First, the size of all its constituent phases: glasses plus euhedral to subhedral crystals (e.g., low-Ca pyroxene [Px1: Wo_4 En_{69} Fs_{27} and Px2: Wo_3 En_{70} Fs_{27}], high-Ca pyroxene [Cpx1: Wo_{43} En_{46} Fs_{11} and Cpx2: $Wo_{41}En_{44}$ Fs_{15}], and chromite [Chr: Cr_2O_3: 45.0 wt%, FeO 31.3 wt%, Al_2O_3: 11.6 wt% and TiO_2: 2.89 wt%]) were adequate for a detail SIMS study (see inset in Fig. 1E showing the ablation pits in each phase). Second, it consists of two glasses with different chemical composition; a Si-Al-Na-rich glass (G1) and a feldspar-like glass (maskelynite?) (G2) (Fig. 1E).

Glassy inclusions vary in size from <10 to 60 μm in diameter, have a subrounded shape, and generally occur in clusters, with a few of them being isolated in olivine grains (Fig. 1F). Both types of inclusions (GI and MIs) can be present in a single olivine grain.

Chemical Composition of Glass Inclusions and Host Crystals

Major Elements

Glassy inclusions in Shergotty are rich in SiO_2 (69–80 wt%) and Al_2O_3 (11–17.4 wt%) and poor in

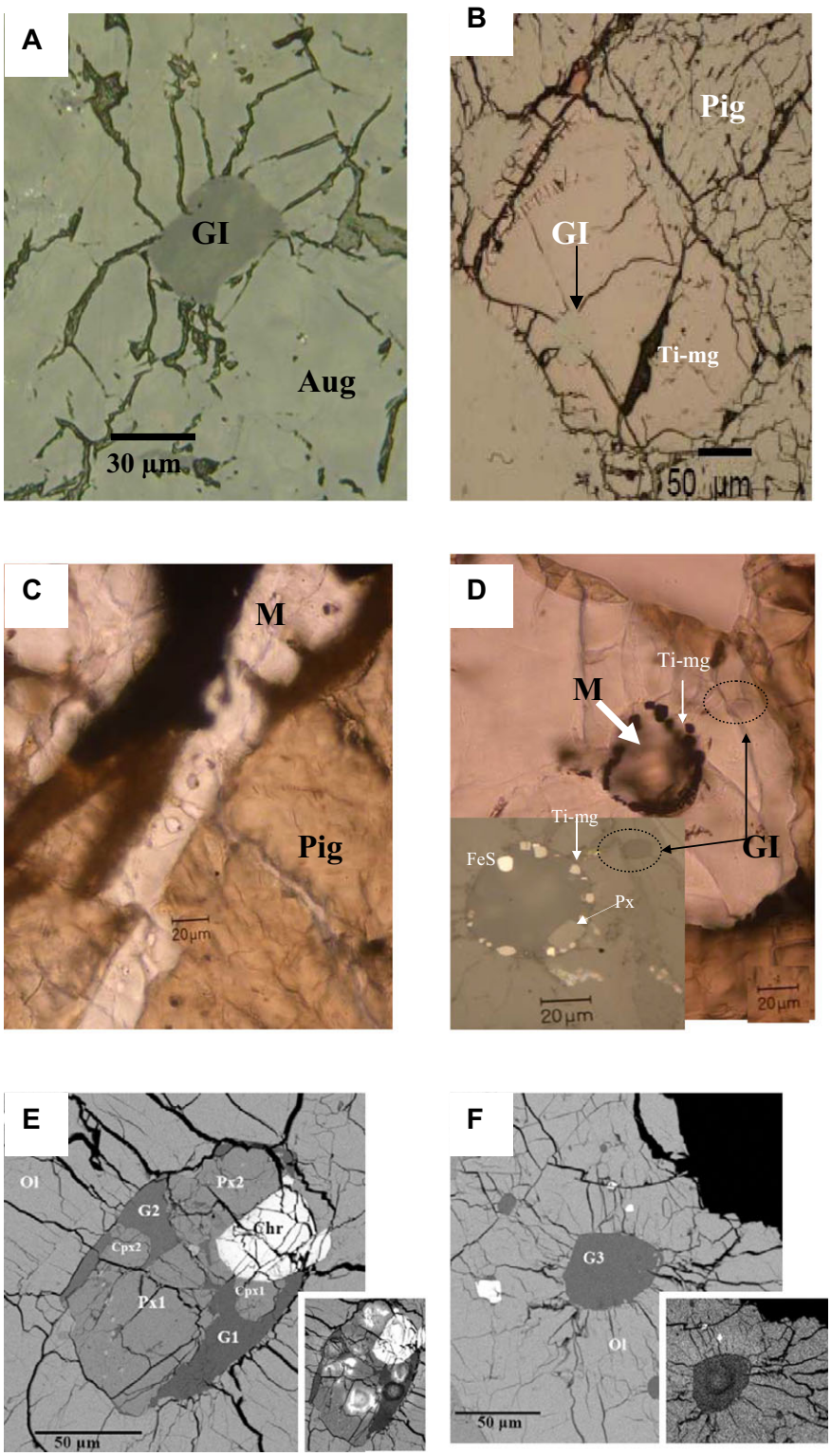

Fig. 1. Photomicrographs of glass-bearing inclusions in Shergotty (A–D) and Chassigny (E, F). Reflective light images of glassy inclusions (GIs): A) in augite (Aug); B) in titanomagnetite (Ti-mg). C) Transmitted light image of round GIs in merrillite (M) that are aligned in the center of the crystal. Note the ~20 µm displacement of the merrillite crystal; D) Transmitted light image of a glassy (GI) and a multiphase inclusion in a euhedral merrillite (M). Details of the different phases inside the MI are shown in the inset (backscattered electron image); E-F) Reflective light images of a multiphase (G1-G2: glass phases; Cpx1-Cpx2: high-Ca pyroxene 1 and 2; Px1-Px2: low-Ca pyroxene 1 and 2, Chr: chromite) and a glassy inclusion (G3), respectively, in Chassigny. Insets show the location of the ablation pits. Note the well developed radial fractures in the host olivine (Ol) surrounding both types of inclusions.

Table 1. Major element chemical compostions of glassy inclusions and host phases in Shergotty.

Glassy inclusions	Pig core B-18[a]		Pig rim		Aug core		Aug rim B-21[a]		M[a]		Ti-mg[a]		Meso	Meso#
N	(2)	SD	(5)	SD	(4)	SD	(2)	SD	(9)	SD	(7)	SD	(3)	(2)
SiO_2	69.0	0.03	73.3	4.6	70.1	0.8	69.5	6.2	74.9	1.3	80.1	2.3	74.8	74.9
TiO_2	0.24	0.06	0.18	0.05	0.28	0.10	0.10	0.05	0.31	0.15	0.39	0.13	0.26	0.53
Al_2O_3	17.4	0.02	14.7	2.0	15.2	0.8	17.9	3.0	12.5	0.8	11.0	1	12.3	12.4
FeO	1.53	0.05	1.41	0.40	1.23	0.09	1.05	0.30	0.94	0.24	1.33	0.37	0.68	1.93
MnO	0.06	0.01	0.05	0.04	0.03	0.02	0.04	0.02	0.03	0.02	0.03			0.03
MgO	0.13	0.04	0.08	0.03	0.06	0.04	0.08	0.05	0.04		0.04			0.08
CaO	1.86	0.03	1.81	0.57	1.49	0.04	1.22	0.03	1.94	0.44	0.60	0.13	0.69	1.60
Na_2O	2.76	0.01	3.72	1.42	2.77	0.42	3.01	0.15	1.26	0.20	1.62	0.73	1.68	1.75
K_2O	6.49	0.15	3.57	2.43	6.57	0.32	7.17	5.00	5.32	0.63	4.18	1.75	7.9	6.11
P_2O_5	0.59	0.07	0.18	0.09	0.15	0.08	0.07	0.02	0.13	0.06	0.11	0.1		
Total	100.0		99.0		97.9		100.1		97.4		99.4		98.3	99.3

Host phases	Pig core	SD	Pig rim	SD	Aug core[a]	SD	Aug rim		M[a]		Ti-mg[a]	
N	(5)		(5)		(7)		(7)	SD	(6)	SD.	(9)	SD
SiO_2	51.4	1.1	47.8	1.0	50.7	1.8	48.0	1.0	0.09	0.02		
TiO_2	0.27	0.13	0.55	0.10	0.54	0.05	0.57	0.05			22.7	1.23
Al_2O_3	1.17	0.60	0.65	0.28	1.83	1.00	0.59	0.13			2.12	0.3
Cr_2O_3	0.28	0.08	0.05		0.40	0.13					0.69	0.69
FeO	21.8	1.3	31.5	1.3	15.6	2.1	33.1	2.5	3.49	0.40	72.7	1.19
MnO	0.72	0.03	1.15	0.63	0.53	0.05	1.14	0.05	0.15		0.53	
MgO	17.9	1.4	10.0		14.1	0.7	6.9	0.7	1.75	0.38		
CaO	6.0	0.6	7.8	1.3	15.2	1.5	9.3	2.0	46.2	0.6		
Na_2O	0.06	0.02	0.07	0.02	0.19	0.04	0.10	0.03	1.40	0.30		
P_2O_5									46.31	1.03		
Total	99.7		99.5		99.1		99.7		99.4		98.7	

Pig. = pigeonite; Aug. = augite; M = merrillite; Ti-mg = titanomagnetite; Meso# = mesostasis analysis from Stolper and McSween (1979).
[a]Phases with SIMS analyses; *N* = number of analyses.

FeO (1.5–0.9 wt%), CaO (2.2–0.6 wt%), and MgO (<0.1 wt%), with variable contents of Na_2O (1.2–3.9 wt %) and K_2O (2.8–7.2 wt%). The chemical composition of GIs hosted in the core and rim of pyroxenes, titanomagnetite and merrillite are shown in Table 1.

GIs trapped by augite and pigeonite cores have similar major element contents (e.g., SiO_2, Al_2O_3 and alkalis [Na_2O + K_2O]). However, those hosted in the rims show highly variable compositions (Fig. 2A). The GIs hosted by merrillite have very similar compositions which, in addition, resemble (except for a small deficit in K_2O) that of the mesostasis (see Meso, Table 1). Similar chemical compositions are also observed in GIs located in the center of elongated euhedral crystals of merrillite and those within curved crystals. The GIs in titanomagnetite show the highest contents of silica, only matched by one inclusion trapped in a pigeonite rim (Fig. 2A).

All glasses (from GIs and MIs) hosted by pigeonite, augite, merrillite, titanomagnetite, as well as the mesostasis, are Cl-free. The major chemical compositions of host phases are given in Table 1.

Glasses in Chassigny (G1, G2, and G3) are silica-rich (64.2 and 73.6 wt%) with highly variable alkali contents (Fig. 2B) as follow. The glassy inclusion G3 has Na_2O and K_2O contents of 6.1 and 1.2 wt%, respectively, whereas in the multiphase inclusion, the glass G1 is Na_2O-rich (12.7 wt%) and the feldspar-like glass G2 (maskelynite?) is Na_2O and K_2O-rich (Na_2O:7.6 wt%, K_2O: 6.9 wt%). Glasses from both GIs and MIs have variable Cl contents with similarly high mean values (Cl —in ppm: GIs 2980 and MIs 2940, Table 2).

Trace Elements

Shergotty

Trace element contents of GIs are highly variable (Figs. 3–5 and Tables 3 and 4). Glasses in Shergotty show high abundances of Zr and Nb (40–5700 × CI and 22–1000 × CI, respectively), with the exception of the GI B-21 hosted in an augite rim (Zr: 5 × CI, Nb: 0.7 × CI).

The variability in the REE content in glasses is largest in the LREE. The GI B-18, located in a

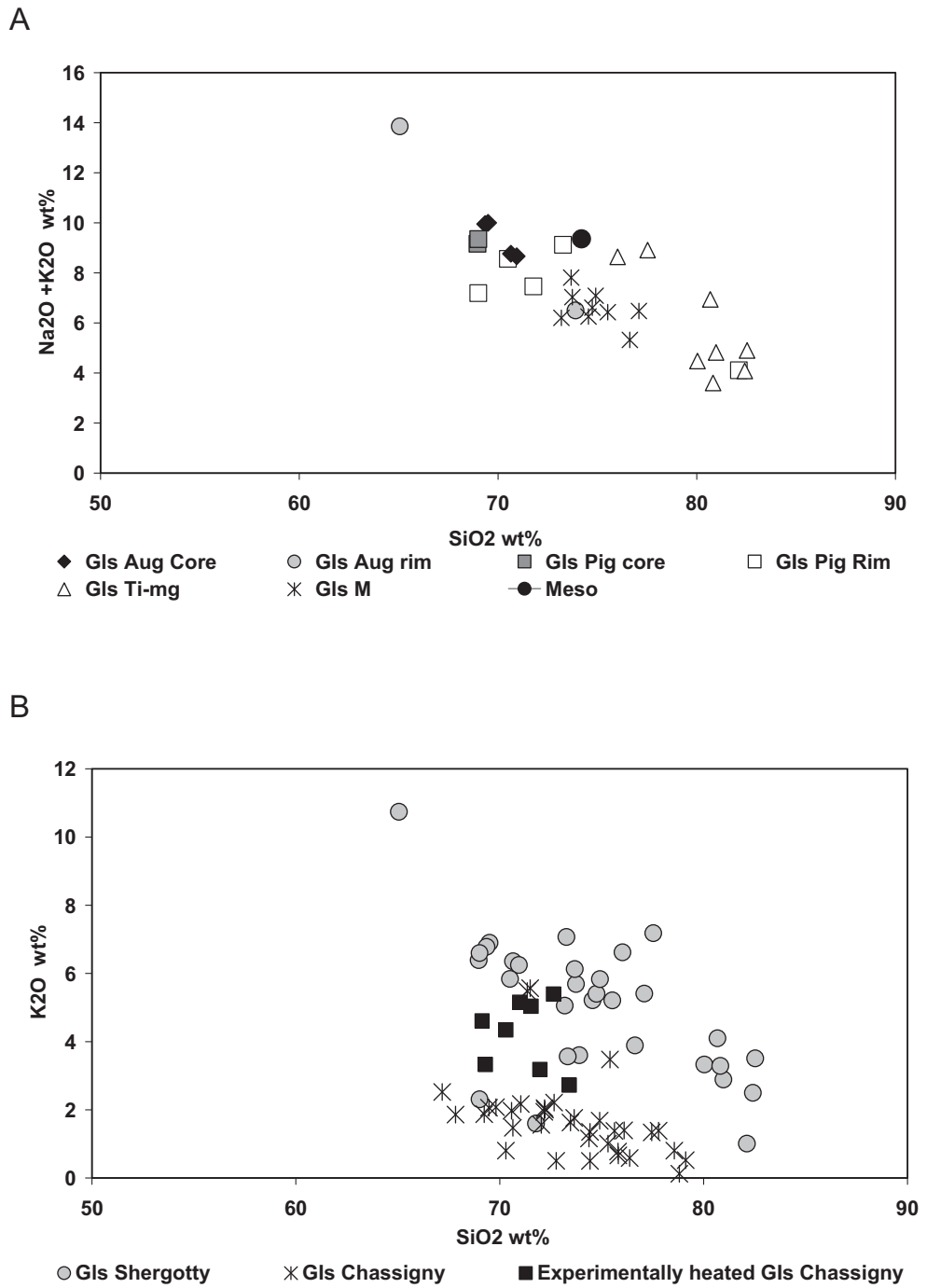

Fig. 2. Major element contents (wt%) in glass inclusions: A) Na_2O+K_2O versus SIO_2 contents in GIs in Shergotty. The composition of mesostasis is given for comparison. B) K_2O versus SiO_2 contents in GIs in Shergotty and the unheated and experimentally heated compositions of glass inclusions in Chassigny (data from Varela et al. 2000).

pigeonite core, has REE contents decreasing with atomic number (La/Lu: ~7) with a negative Eu anomaly (8 × CI). The glasses trapped by the augite rim (B-21) and by a titanomagnetite show a fractionated LREE-depleted pattern (La/Lu: 0.15 for B-21 and 0.5 for the GI in titanomagnetite; Fig. 3). As indicated above, three inclusions (2 GIs and 1 MI) trapped by merrillite are contaminated and therefore their REE contents were not considered. These inclusions have glasses with high abundances of Sr and Ba (from ~10 × CI to ~100 × CI, respectively) as well as very high contents (>100 × CI) of Rb.

Table 2. Major element chemical composition of glasses and co-existence phases in a multiphase and glassy inclusion in Chassigny.

	Multiphase inclusion								Multiphase inclusion		Glassy inclusion		Glassy inclusion		Mesostasis[a]	
N	G1[a] (2)	G2 (Msk?)[a] (2)	Cpx1[a]	Cpx2[a]	Px1[a]	Px2[a]	Chr[a]	Ol-host[a]	Glass (12)	SD	G3[a] (3)	Ol-host[a]	(35)	SD	(4)	SD
SiO_2	64.2	64.2	49.3	50.4	52.3	52.3	0.0	37.1	68.2	3.40	73.6	37.0	73.4	3.08	61.9	0.9
TiO_2	0.06	0.08	1.24	0.94	0.48	0.44	3.39	0.02	0.20	0.08	0.23	0.02	0.17	0.08	0.1	0.08
Al_2O_3	22.3	20.8	4.7	4.0	2.8	3.2	12.9	0.0	18.2	1.83	18.0	0.0	17.6	1.11	24.3	1.7
Cr_2O_3	0.00	0.00	1.00	0.34	0.28	0.34	45.2	0.05	0.02	0.03		0.02	0.03	0.02		
FeO	0.50	0.60	8.0	8.6	17.1	16.7	32.9	28.2	0.68	0.18	0.63	28.0	1.24	0.91	0.6	0.12
MnO	0.00	0.00	0.33	0.36	0.59	0.48	0.52	0.50	0.02	0.03	0.02	0.52	0.04	0.04		
MgO	0.02	0.00	14.8	14.7	24.5	24.7	3.93	34.4	0.07	0.15	0.04	34.3	0.31	0.61	0.04	
CaO	0.27	0.04	19.2	19.2	1.93	1.60	0.00	0.17	0.51	0.41	0.80	0.14	0.60	0.26	4.64	0.37
Na_2O	12.7	7.6	0.48	0.45	0.00	0.00	0.00	0.00	8.1	1.22	6.1	0.00	4.43	3.08	7.06	1.35
K_2O	0.25	6.9	0.00	0.00	0.00	0.00	0.00	0.00	3.23	2.04	1.20	0.00	1.71	1.16	1.03	0.45
Total	100.3	100.2	99.1	99.0	100.0	99.7	98.8	100.4	99.3		100.6	100.0	99.6		99.7	
Cl (ppm)	500	3700							2940	736	2580		2980	1128		

G1-G3 = glass phases; G2(Msk?) = maskelinite?; Cpx1-Cpx2 = high-Ca pyroxene 1 and 2; Px1-Px2 = low-Ca pyroxene 1 and 2, Chr = chromite; Ol-Host = host olivine.
[a]Phases with SIMS analyses; *N* = number of analyses.

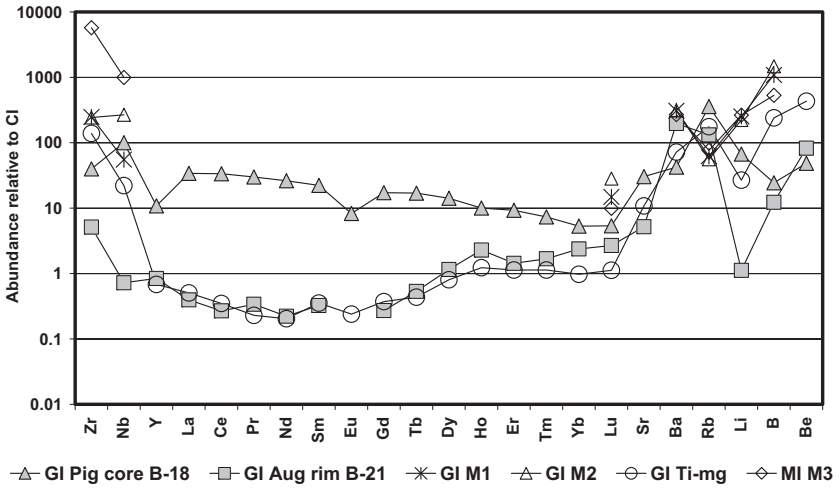

Fig. 3. CI-normalized (Lodders and Fegley 1998) trace element abundances in glasses of GIs in Shergotty. In this and the following figures the elements are arranged in order of falling 50% condensation temperature (Lodders 2003), except the REE, which are arranged in order of increasing atomic number.

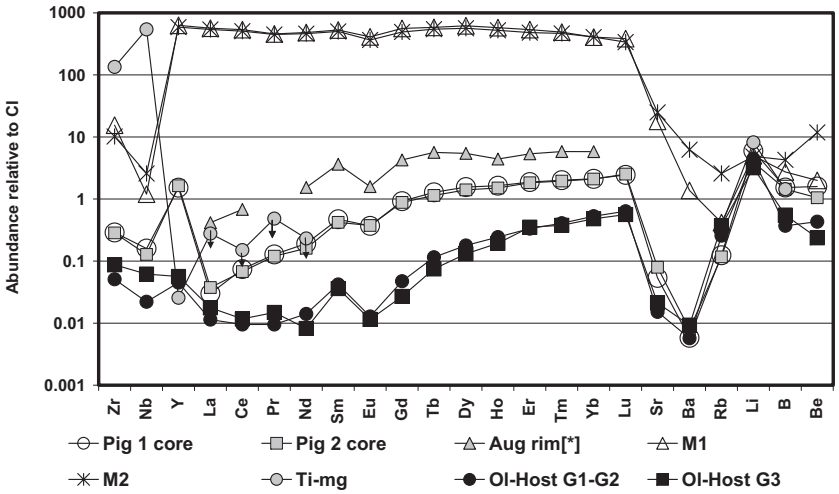

Fig. 4. CI-normalized trace element abundances of host minerals of glass inclusions in Shergotty and Chassigny. Aug rim [*] is from Wadhwa and Crozaz (1995).

All GIs show high abundances of Be, varying from ~50 × CI (GI B-18 in the pigeonite core) to 1400 × CI (GIs in merrillites). Abundances of B and Li are also variable, with the GI located at the augite rim being less enriched (B: 12 × CI; Li: 1 × CI) than the GIs hosted by late phases (B: 240 × CI, Li: 25 × CI, Fig. 3). The GI located in the pigeonite core shows similar abundances of Li (55 × CI) and Be (48 × CI) and a low content of B (24 × CI) (Fig. 3).

Trace element contents of host phases (pigeonite, titanomagnetite, and merrillite) are similar to those previously reported (e.g., Wadhwa et al. 1994) (Fig. 4). The LREE contents of titanomagnetite (~0.2 × CI) are higher than those of the HREE (as inferred by the Y abundance of 0.03 × CI, Table 3). All host phases show very similar contents in Li (~7 × CI), B (~3 × CI) and Be (~1 × CI, with exception of W2) (Fig. 4).

Chassigny

Glasses have high abundances in Zr (20–190 × CI) and Nb (40–1000× CI) (Fig. 5). The REEs in the glassy inclusion (G3) have a highly fractionated LREE-enriched (La/Lu: 44) pattern. The glass G1 in the multiphase inclusion is REE-poor and has a slightly fractionated, LREE-enriched (La/Lu: 1.8) pattern with negative abundance anomalies of Tb (0.24 × CI). The feldspar-like glass G2 shows a flat pattern slightly enriched in HREE (La/Lu: 0.62) with REE abundances around 3 × CI (Fig. 5).

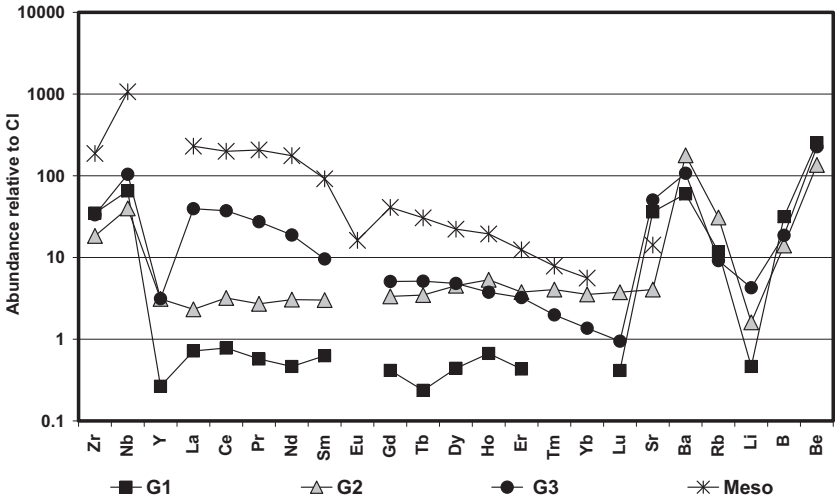

Fig. 5. CI-normalized trace element abundances of glasses in a multiphase inclusion (G1 and G2), in a glassy inclusion (G3), and in mesostasis (Meso) in Chassigny.

Glasses G1 and G3 show high contents in Sr (50 × CI), Ba (~80 × CI), and Rb (~10 × CI). The feldspar-like glass (G2) matches the G1 and G3 glasses in their Ba and Rb contents, but is poor in Sr (~5 × CI) (Fig. 5). The mesostasis has a fractionated LREE-enriched pattern (normalized La/Yb: 38) with a negative anomaly in Eu (~10 × CI) as compared to the geometric mean of the Sm and Gd abundances (~60 × CI); a similar pattern to glassy inclusion G3 (normalized La/Lu: 40), but with REE abundances higher by about one order of magnitude (Fig. 5). All glasses show Li contents of ~2 × CI and increasing abundances of B (~25 × CI) and Be (~250 × CI) (Fig. 5).

Among the different phases present in MI, the high-Ca pyroxenes (Cpx1 and Cpx2) have similar contents of Zr and Nb (~20 × CI) and high (10–50 × CI) REE abundances (Fig. 6). Both high-Ca pyroxenes differ slightly in their normalized La/Lu ratios and have similar abundances of Li (1.6 × CI), B (8 × CI), and Be (70 × CI), but differ in their Ba contents. The low-Ca pyroxene Px1 shows a fractionated REE pattern with a normalized La/Lu ratio of 0.067 (La: 0.27 × CI, Lu: 4 × CI, Fig. 6). The pyroxene Px2 shows a fractionated pattern with the LREEs being enriched over the HREEs and a normalized La/Lu ratio of ~6 (La: 51.7 × CI; Lu: 8.4 × CI, Fig. 6), which is similar to an amphibole pattern A close inspection after SIMS analysis shows the presence of an amphibole-like phase (SiO_2: 50.9 wt%, Al_2O_3: 2.24 wt%, MgO: 19.3 wt%, CaO: 11.2 wt%, FeO: 12.6 wt%, Na_2O: 0.33, K_2O: 0.03 wt%, and P_2O_5: 1.8 wt%) between the border of the inclusion and Px2. Although the SIMS analysis was performed some tenths of micrometers away from this amphibole-like phase, we cannot exclude some intergrowth and trace element contamination as REE contents remained high and constant throughout the SIMS analysis of Px2.

The trace element contents of the host olivine crystals are low and are given in Table 4 and shown in Fig. 4.

DISCUSSION

The chemical compositions of the SNC meteorites' parent magmas, estimated from modal abundances and average compositions of constituent phases on primary glass-bearing inclusions or from results of experimental heating experiments, range from basaltic to dacitic (e.g., Varela et al. 2001; Stockstill et al. 2005; Treiman 2005; McCubbin and Nekvasil 2008; Goodrich et al. 2013).

A recent study of glass-bearing inclusions in Chassigny indicated that the melt trapped during the growth of the olivine was alkali in composition, similar to a hawaiite of the silica-saturated alkalic variety (Nekvasil et al. 2007). The crystallization process of the meteorite seems to have taken place under elevated pressures, as suggested by the chemical composition of feldspar pairs and kaersutite within MIs (McCubbin et al. 2007; McCubbin and Nekvasil 2008).

A different scenario was proposed by Varela et al. (2000) in which MIs in Chassigny olivine are considered to be the result of heterogeneous entrapment. Consequently, the crystals inside inclusions are not considered to be daughter crystals formed as the product of postentrapment closed-system evolution of an originally homogeneous melt. Accordingly, the compositional variability observed in glasses and the constituent phases of these glass-bearing inclusions indicate that olivine crystals have trapped heterogeneous

Table 3. Secondary ion mass spectrometry (SIMS) analyses of glasses and host phases (ppm) in Shergotty (detailed errors are given only if they are larger than 10%).

	GIs								MI	Host phases								
	Pig core B-18	Error	Aug rim B-21	Error	M1	M2	Ti-mg	Error	M3	Pig 1 core	Error	Pig 2 core	Error	M1	Error	M2	Ti-mg	Error
Li	100		1.7		94	84	40		114	8.9		5.9		7.5		7.3	12	
Be	1.2		2		27	37	11		13	0.04		0.07		0.05		0.3	2.5	
B	21		10.7		220	193	208		229	1.33		1.25		2.4		3.7	1.25	
Rb	823		303		708	715	404		618	0.28	0.04	0.27	0.09	0.96	0.098	6	0.86	
Sr	236		40.6		117	220	84		78	0.42		0.62		139		194	7.2	
Y	17		1.3		15	474	1.1		10	2.37		2.6		982		917	0.04	0.0045
Zr	156		20.5		915	898	546		21200	1.14		1.12		61		40	530	
Nb	24		0.18	0.02	14	67	5.4		249	0.04		0.03		0.3		0.6	133	
Ba	99		460		214	44	168		79	0.01	0.002	0.02	0.003	3.2		14	6.7	
La	8		0.09		2.3		0.1			0.007	5E-04	0.009	0.002	133		126	0.06	0.009
Ce	20		0.16	0.017			0.2			0.05		0.04		323		306	0.09	0.01
Pr	2.7		0.03	0.004			0.02	0.002		0.01		0.01		41		39	0.04	0.006
Nd	12		0.1				0.09			0.08		0.07		218		209	0.1	
Sm	3.3		0.05	0.01			0.05	0.009		0.07		0.06		77		74		
Eu	0.5	0.07					0.01	0.08		0.02		0.02		23		20		
Gd	3.4		0.05	0.01			0.07	0.008		0.18		0.17		110		96		
Tb	0.6		0.02	0.003			0.016	0.002		0.05		0.04		21		20		
Dy	3.4		0.28	0.02			0.2			0.38		0.34		150		137		
Ho	0.6		0.13	0.016			0.07			0.09		0.08		32		29		
Er	1.5		0.23				0.18			0.3		0.3		85		76		
Tm	0.18		0.04	0.01			0.03	0.005		0.05		0.05		12		11		
Yb	0.9		0.38				0.16			0.34		0.34		66		66		
Lu	0.13	0.02	0.07	0.01			0.03	0.004		0.06	0.006	0.06	0.009	9.4		8.2		

GIs = glassy inclusions; MI = glass in multiphase inclusion; Aug. = augite; Pig = pigeonite; M = merrillite; Ti-mg = titanomagnetite.

Table 4. Secondary ion mass spectrometry (SIMS) analyses of glasses, host phases, and minerals (ppm) in Chassigny (detailed errors are given only if they are larger than 10%).

	Glasses							Host phases				
	G1	Error	G2	Error	G3	Error	Mesostasis	Error	Ol G1-G2	Error	Ol G3	Error
Li	0.73		2.5		6.7				7		5	
B	31		14		18				0.36		0.54	
Be	7		3.66		6				0.01		0.006	
Rb	27		71		21				0.6	0.08	0.85	0.09
Sr	286		32		400		110		0.12		0.17	
Y	0.4		4.84		4.9		20		2.7		3.4	
Zr	129		68		123		738		0.19		0.32	
Nb	16		10		26		263		0.006	0.001	0.015	0.0015
Ba	136		403		243				0.013	0.002	0.02	0.002
La	0.17	0.017	0.55	0.06	9.3		54		0.003	0.0007	0.004	0.0008
Ce	0.48		1.97		23		120		0.006	0.0007	0.007	0.001
Pr	0.05	0.006	0.25	0.04	2.5		18		0.0009		0.001	0.0003
Nd	0.21		1.4		8.6		80		0.007	0.0009	0.004	0.0007
Sm	0.09	0.01	0.45	0.08	1.4		13.5		0.007	0.001	0.005	0.001
Eu							0.9	0.12	0.0007		0.0006	
Gd	0.08	0.01	0.66	0.09	1	0.2	8		0.009	0.001	0.005	0.001
Tb	0.008	0.002	0.12	0.02	0.2	0.03	1.1	0.11	0.004	0.0005	0.003	0.0004
Dy	0.11		1.1		1.2		5.4		0.04		0.03	0.001
Ho	0.04	0.005	0.3	0.03	0.2	0.02	1.1		0.01	0.001	0.01	0.001
Er	0.07	0.009	0.6	0.06	0.5		2		0.05		0.06	
Tm			0.1	0.02	0.05	0.008	0.19	0.04	0.01	0.001	0.009	0.0009
Yb			0.56	0.06	0.22	0.04	0.91	0.1	0.08		0.08	
Lu	0.01	0.003	0.09	0.02	0.02	0.009			0.02	0.002	0.01	0.001

	Phases in the multiphase inclusion									
	Cpx1	Error	Cpx2	Error	Px1	Error	Px2	Error	Chr	Error
Li	1.9		3		1.96		1.6		2	
Be	1.5		2		0.27		0.5		0.03	
B	6.4		9.4		1.04		3		0.2	0.02
Rb			16		0.9	0.2			0.26	0.03
Sr	195		89		2.6		170		0.53	
Y	32		41		5.5		19		0.26	
Zr	71		80		7.6		15		1.7	
Nb	3.9		2.4		0.3		0.6		0.45	
Ba	9.8		82		3.5		9.2		0.65	
La	2.7		3.3		0.06	0.006	12		0.03	0.005
Ce	15		16.7		0.25		35		0.14	0.016
Pr	3.5		3.6		0.06	0.007	4.9		0.03	
Nd	18		20		0.44		21		0.16	
Sm	6.3		7.6		0.25		5.1		0.07	0.01
Eu	1.2		1.6		0.07	0.007	1.5		0.01	0.002
Gd	7.5	0.8	8.5		0.5	0.05	4.5		0.07	0.01
Tb	1.1	0.17	1.6		0.12	0.012	0.7	0.076	0.01	0.002
Dy	8.4		8.6		0.9		4.4		0.06	0.008
Ho	1.26	0.14	1.6		0.25	0.026	0.72		0.02	
Er	3.3		3.8		0.6		1.9		0.03	0.004
Tm	0.39	0.06	0.4	0.04	0.1		0.17	0.026	0.03	
Yb	1.7	0.3	1.9	0.3	0.6	0.08	1.1	0.154	0.02	0.004
Lu	0.28	0.06	0.14	0.05	0.1		0.2	0.04	0.01	

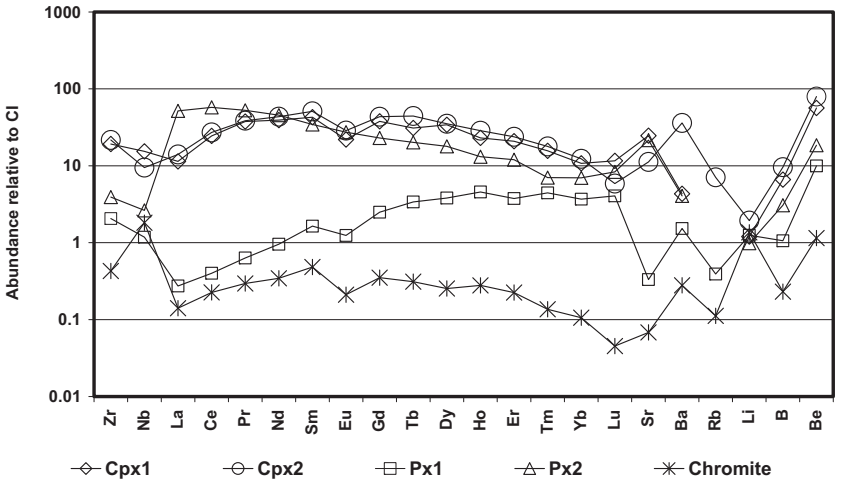

Fig. 6. CI-normalized trace element abundances of the different phases inside a mutiphase inclusion in Chassigny: high-Ca pyroxenes: Cpx1 and Cpx2; low-Ca pyroxenes: Px1 and Px2, and chromite.

phases, possibly precipitates of a fluid/melt that existed during formation of Chassigny constituents.

Recent data from experimentally rehomogenized melt inclusions from lherzolitic shergottites, combined with previously calculated fO_2 values for the basaltic shergottites, indicate a range in fO_2 of four orders of magnitude. Although the reason for this range is not well understood, it appears to require multiple processes such as mineral/melt fractionation, assimilation, and/or shock (McCanta et al. 2009). Clearly, although extensive detail studies are performed in these glass-bearing inclusions, the answers are far from being straightforward, but rather puzzling.

Although these inclusions are assumed to represent pristine samples of melts/liquids that formed in thermodynamic equilibrium with their host minerals, their study is difficult.

On the one hand, such inclusions are not very abundant. In previous investigations, the number of studied inclusions was significantly restricted. Several of these inclusions (e.g., the small pure glass inclusions <25–30 μm) were excluded under the assumption that they were not representative samples (Harvey and McSween 1992; Treiman 1993) because boundary layer effects could cause their bulk compositions to deviate from that of the initially trapped liquid. However, the study of all types of inclusions in Chassigny (Varela et al. 2000) showed that small GIs can give important information and should not be neglected. Later dynamic forsterite crystallization experiments (Faure and Schiano 2005) showed that the melt trapped in glass inclusions is representative of the bulk melt irrespective of the size of the inclusion. Recently, studies of the olivine-phyric shergottite Tissint (Sonzogni and Treiman 2013) gave additional support to this view and concluded that both small and large inclusions should be taken into account.

On the other hand, their pristine chemical composition can be substantially modified, considering that most of the SNC meteorites appear to have cooled slowly and experienced some degree of subsolidus chemical equilibration (e.g., McSween 1985, 1994; Mittlefehldt 1994; Treiman et al. 1994). This fact raises some concern that these inclusions may have their initial melt compositions modified by diffusive exchange processes during and after entrapment. In addition, shergottites and chassignites were affected by shock-induced metamorphism (El Goresy et al. [2013] and references therein). Therefore, it is important to elucidate the extent to which these inclusions have remained as consistent (unmodified?) samples of the originally trapped melt.

In the following sections, we discuss our findings in the light of latest results.

Chemical Compositions of Glasses

Alkali Abundance

Normative calculations of glasses from GIs and MIs in Shergotty indicate that they are dominated by Qz-Or-Ab, with minor An and minor pyroxene (ferrosilite from 1.3 to 2.7%) component. Projected onto the plane orthoclase (Or)-albite (Ab)-anorthite (An), the GIs' compositions fall onto the trend defined by the mesostasis in Shergotty (Stolper and McSween 1979).

All liquids/melts are SiO_2 enriched and their alkali contents ($Na_2O + K_2O$) display a negative correlation with SiO_2 (Figs. 2A and 2B). The alkali contents of GIs trapped in the core of both types of pyroxenes (pigeonite and augite) are fairly similar. However, GIs

trapped in their rims are highly variable, both higher and lower than those GIs located in the cores. If glasses were the residua after crystallization of a melt that is evolving in a closed system, we might expect a positive correlation, with the final stage of evolution showing the highest content of Na_2O. The decrease in the alkali content ($Na_2O + K_2O$) is too large to be attributed to a dilution effect.

In Chassigny, GIs are mainly trapped in olivine. Their Na_2O and K_2O contents are negatively correlated with the SiO_2 content (Fig. 2B). Previous studies using micro-PIXE and nuclear reaction analysis (NRA) showed that glass-bearing inclusions in Chassigny hosted in a single olivine have highly variable nitrogen (N) and Rb/Sr ratios, with glasses in one and the same inclusion showing chemical inhomogeneity (e.g., variation in element distribution with depth) (Varela et al. 2000). This nonhomogeneous glass composition and the compositional variability of Na, K, halogens, Rb, Sr, and N in glasses from all types of inclusions (glassy, monocrystal, and multiphase) suggest that glass inclusions could be the result of trapping or mixing of chemically heterogeneous phases (e.g., crystalline phases and fluids) that existed shortly before or at the moment of the inclusions' formation (Varela et al. 2000). Alternatively, as discussed below, the compositional variability in these inclusions could be the result of a significant disturbance produced by late processes that mobilized these elements.

Similar large variations in Na_2O and K_2O in glasses within different glass-bearing inclusion types from olivine-phyric shergottites were also described (e.g., Goodrich 2003; Basu Sarbadhikari et al. 2011). Also, the presence of K-rich glass and Na-rich glass within a single glass-bearing inclusions was recently described in the ferroan chassignite NWA 8694 (Hewins et al. 2015). Despite the numerous detailed studies, the nature of the mechanism that caused these large abundance variations (mainly that of K_2O) remains a matter of debate.

In summary, the chemical variability observed in glass inclusions in Shergotty and Chassigny are different. In the latter all types of inclusions (trapped in core and rim of olivine crystals) record inhomogeneities and chemical variability (e.g., Na, K, Rb). In Shergotty, the GIs trapped in the core of both types of pyroxenes (pigeonite and augite) have similar major element contents (e.g., SiO_2, Al_2O_3 and alkalis [$Na_2O + K_2O$]). However, those trapped in their rims show highly variable alkali contents, both higher and lower than those of GIs located in the cores.

In the following section, we show that this variability is not restricted to their major element contents but also to their trace element abundances.

Trace Element Abundances

Shergotty

The GI B-18 located in a pigeonite core (GI Pig. Core B-18, Fig. 7A) is out of equilibrium with its host phase, as revealed by its trace element abundances. Addition of variable percentages (e.g., 10%, 20%, or 40%) of the wall phase (Pig. 1 core, Table 3, Fig. 4) to the glass will not restore the equilibrium. For example, by adding an unrealistic 40% of the pigeonite host the REE contents of GI B-18 will slightly increase the HREE ~0.7 × CI with a small depletion in the LREE abundances (<0.2 × CI; see GI-B18 + 40% host, Fig. 7A). The liquid in equilibrium with the pigeonite core was calculated using the trace element partition coefficients from Lundberg et al. (1988). The liquid (L. Equil. Pig Core, Fig. 7A) is enriched in HREE (Er and Yb) and strongly depleted in LREE as compared to GI B-18 and GI B-18 + 40% host. Also, the REE abundances of GI B-18 differ from those of the calculated 70% intercumulus melt (70% ICM, Fig. 7A) (Lundberg et al. 1988). At this melt proportion, the equilibrium composition of pyroxenes in experimental Shergotty melts is identical to those of homogeneous pyroxene cores in Shergotty (Stolper and McSween 1979).

However, for GI B-21 hosted in the augite rim, the calculated liquid in equilibrium with the host (L. Equil. Aug rim, Fig. 7A) shows LREE (La–Nd) ~20 × CI, and HREE (Sm-Yb) ~40 × CI, which are one to two orders of magnitude lower (Fig. 7A). This depletion in REE contents is surprising. If GIs represent small amounts of late residual liquids (as revealed by their major element composition), their REE contents should be similar to those of late-stage interstitial melt. However, none of the GIs (e.g., GIs trapped by late phases such as titanomagnetite) have trace element contents that resemble those of the K-rich glasses or the late-stage interstitial melt (Lundberg et al. 1988) (Fig. 7B).

When comparing major and trace element compositions of GIs trapped in the core and rim of pyroxenes we are faced with an interesting situation: they have similar major element concentrations (compare B-21 and B-18, Table 1), but very different trace element contents. The GIs B-21 and B-18 have LREEs abundances that differ by up to two orders of magnitude, with patterns showing opposite (B-18: La/Lu:~7; B-21: La/Lu: 0.15) fractionations (Figs. 3 and 7A). Although we cannot rule out that variable volumes of host pyroxene may have precipitated onto B-21 and B-18 inclusions' walls during cooling, this cannot account for the differences in the LREE abundances. Conversely, glasses with different major element compositions, such as those trapped in a late stage of crystallization, either

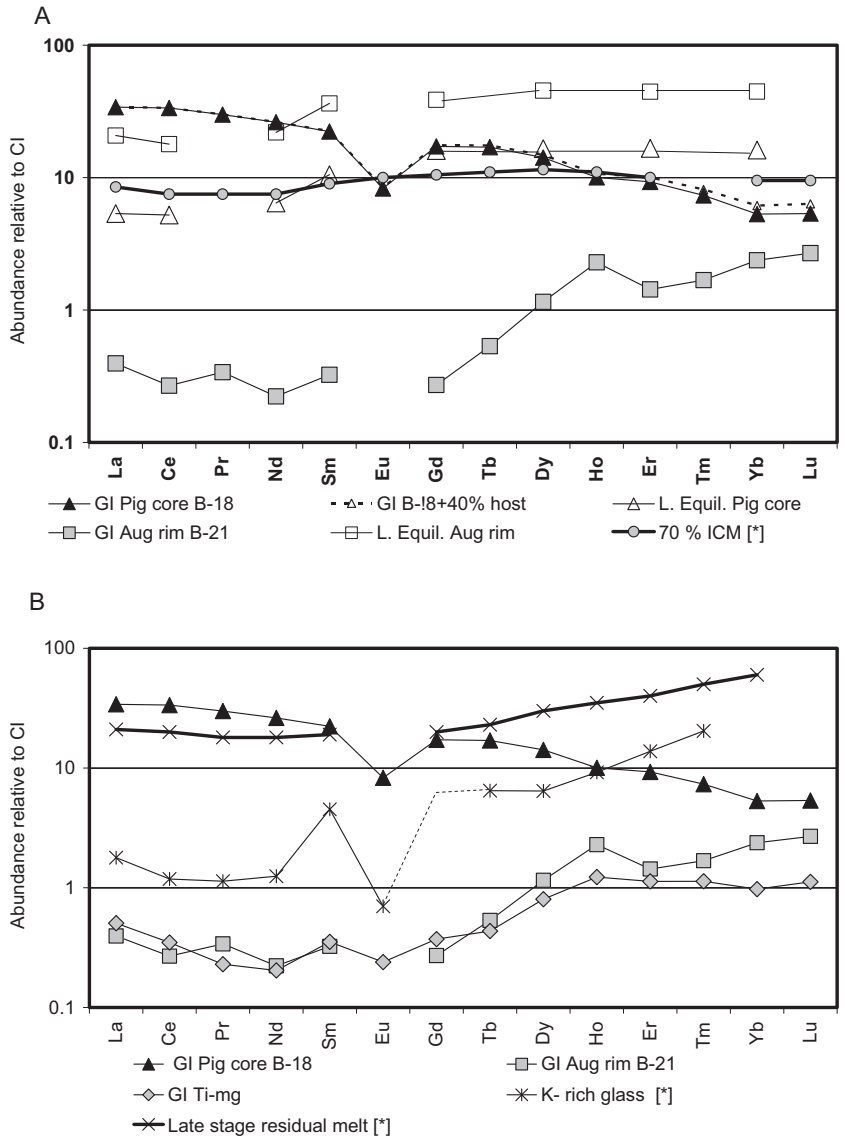

Fig. 7. CI-normalized REE abundances of GIs in Shergotty. A) Of GIs trapped in a pigeonite core (GI Pig Core B-18), in an augite rim (GI Aug rim B-21), and the calculated liquids in equilibrium with the host minerals (L. Equil. Pig core and L. Equil. Aug rim). The REE contents of the calculated 70% intercumulus melt (70% ICM) from Lundberg et al. (1988) is given for comparison. B) The REE contents of all GIs of this study are compared to those of a K-rich glass from Shergotty and the calculated late residual melt from Lundberg et al. (1988).

hosted by the augite rim (B-21) or by the titanomagnetite (Ti-mg, see Table 1), show similar fractionated LREE-depleted patterns (Figs. 3 and 7A).

The existence of LREE-rich and LREE-poor glasses could suggest that some inclusions were trapped before or after the onset of phosphate formation. However, considering that the phosphate is a late phase, the trace elements abundances of glass inclusions trapped by the augite rim (B-21) and in titanomagnetite should be REE-rich. The late REE-rich phases need a REE-rich liquid, consequently also a REE-rich late-stage residual melt, similar to those of the late-stage residual melt from Lundberg et al. (1988) (Fig. 7B). But, this is not what we observed.

Regarding the light lithophile elements (LLE), although we could not find a GI in an augite core suitable for SIMS analysis, data from GI B-18 can be used, as both pyroxenes (augite and pigeonite) are early cocrystallizing phases in Shergotty (McSween 1994) and have similar Li zoning (Herd et al. 2005). The almost two orders of magnitude lower Li content of B-21 (augite rim) compared to B-18 (pigeonite core, Fig. 3) appears to support exsolution and loss of Li by aqueous fluids (Lentz et al. 2001; McSween et al. 2001). With a

partition coefficient $D_{Li\ (pyroxene)}$ of 0.2 (Herd et al. 2004), the melt in equilibrium with pyroxene cores (Li contents of 5.9–8.9 ppm, Table 3) should have ~30–44 ppm Li. However, the trapped liquid/melt in B-18 has more than twice the expected Li content. If we assume a Li content of ~1.5 ppm for the augite rim (Herd et al. 2005), the co-existing melt should have ~7.5 ppm Li. B-21 has 1.7 ppm Li, which is only a quarter of the expected amount. Such a strong depletion in Li points toward its loss after core crystallization. However, if Li is lost from the basalt via aqueous fluids, B will follow Li (Lentz et al. 2001) and, therefore, both elements should show a similar behavior. However, the small difference in B abundances as recorded in B-18 and B-21 is not consistent with this scenario (Fig. 3). Our data show a large variation in Li coupled with a slight variation of B, and are in agreement with latest results about Li and B distribution in pyroxene. Herd et al. (2005) show that Li concentrations in pyroxene decrease from cores to rims by a factor of 4 in Shergotty while B zoning is ambiguous.

The liquids/melts trapped in GIs hosted by merrillite are also highly enriched in Li. Their partition coefficients $D_{Li\ (merrillite)}$: ~0.06 are 10 times lower than experimentally constrained values ($D_{Li\ (merrilite)}$:0.7, see table 1 of Treiman et al. [2006] and references therein). Therefore, the variable light lithophile element contents of GIs do not seem to be a direct result of the crystallization event. Because Li is one of the fastest elements for solid state diffusion (Giletti and Shanahan 1997) the pristine Li distribution inherited from magmatic processes could be strongly perturbed due to the strong mobility of Li in mineral phases.

Most likely, the large variation in Li, as those observed in this study, could be the result of postformational processes, such as shock-induced diffusion (Beck et al. 2004) or metasomatism.

In summary, the chemical composition of the GIs in Shergotty reveal an unusual geochemistry in which glasses of GIs are out of equilibrium with their host crystals with trace element contents that appear to be independent of their major element contents. Their LREE abundances differ by up to two orders of magnitude, with patterns revealing opposite fractionations (B-18: La/Lu: ~7; B-21: La/Lu: 0.15) and late-stage liquid extremely depleted in REE (residual melts trapped by GIs in rims and late phases). In addition, all GIs show highly variable light lithophile element contents.

The chemical compositions of these glass-bearing inclusions appear to have been highly disturbed.

Chassigny

A similar situation is observed in GIs and MIs in Chassigny. Trace and minor element study of constituent phases in this meteorite (Wadhwa and Crozaz 1995) show that the parent melt of Chassigny was LREE enriched and that the whole rock can be explained by closed-system fractionation from a melt similar in composition to the trapped melt in the cumulus pile. The liquid in equilibrium with the late-formed minerals in Chassigny has a trace element pattern parallel to that of the whole rock and also to the calculated parent melt (Wadhwa and Crozaz 1995).

Glass-bearing inclusions are considered to represent assemblages equivalent to those present in terrestrial igneous rocks, hence mineral phases inside glass-bearing inclusions are assumed to have formed during the cooling of an initially trapped melt (e.g., daughter minerals). However, crystalline phases inside the MIs in Chassigny did not dissolve in the melted glass during heating experiments (Varela et al. 2000), suggesting that glasses may not be a residual phase after closed-system crystallization.

Our trace element study of the different mineral phases in glass-bearing inclusions revealed some unresolved problems.

If we apply the experimentally determined distribution coefficients of trace elements between olivine and glass (McKay and Weill 1977; Kennedy et al. 1993; Green 1994; Lodders and Fegley 1998), we observe that the glass of the glassy inclusion G3 is out of equilibrium with its host olivine (Fig. 8A). A similar lack of equilibrium is present between the different crystal phases inside the multiphase inclusion (Fig. 1E). Px1, Cpx1, and G1 are out of equilibrium as are Cpx2 and G2. The low- and high-Ca pyroxenes (Px1, Px2, Cpx1, Cpx2) are calculated to be in equilibrium with different liquids that are highly enriched in all trace elements compared to those observed in the co-existing glasses (Fig. 8B). This lack of equilibrium poses a problem and suggests that glass (or their precursors) and crystal phases inside the multiphase inclusion cannot be an assemblage of melt + daughter minerals formed by closed-system crystallization from an originally homogeneous melt.

Also, the depletion in trace element abundances of G1 is inconsistent with this phase being a residual melt after crystallization of low-Ca and high-Ca pyroxenes inside the multiphase inclusion (Px1-2 and Cpx 1-2, respectively, Fig. 1E). G1 should be enriched in its trace element contents, similar to what is observed for the mesostasis (Fig. 5). Surprisingly, the REE element abundances of G1 are even lower than those calculated for melts in equilibrium with early and late phases in Chassigny (Wadhwa and Crozaz 1995; Fig. 8C), which is a geochemical impossibility.

Another interesting phase is the feldspar-like glass G2 (Fig. 5), which resembles maskelynite due to its

A

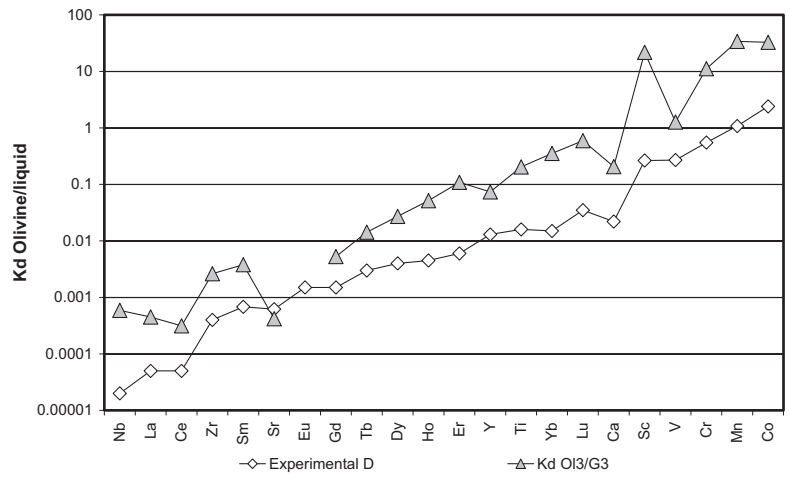
Kd Olivine/liquid
100
10
1
0.1
0.01
0.001
0.0001
0.00001
Nb La Ce Zr Sm Sr Eu Gd Tb Dy Ho Er Y Ti Yb Lu Ca Sc V Cr Mn Co
Experimental D
Kd Ol3/G3

B

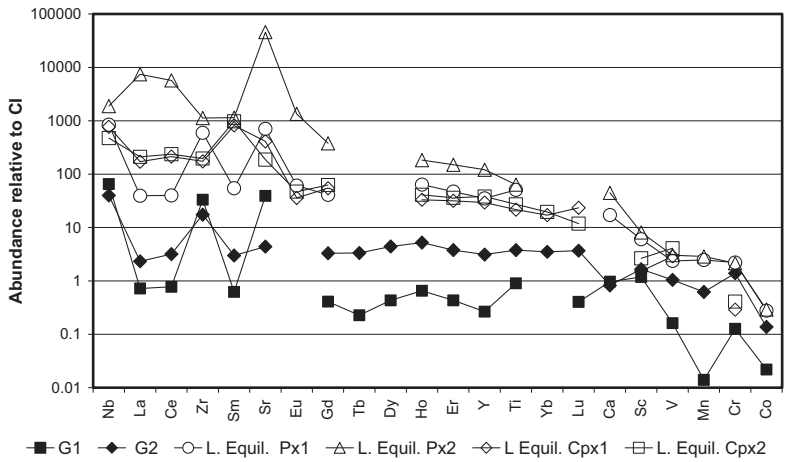
Abundance relative to CI
100000
10000
1000
100
10
1
0.1
0.01
Nb La Ce Zr Sm Sr Eu Gd Tb Dy Ho Er Y Ti Yb Lu Ca Sc V Mn Cr Co
G1
G2
L. Equil. Px1
L. Equil. Px2
L Equil. Cpx1
L. Equil. Cpx2

C

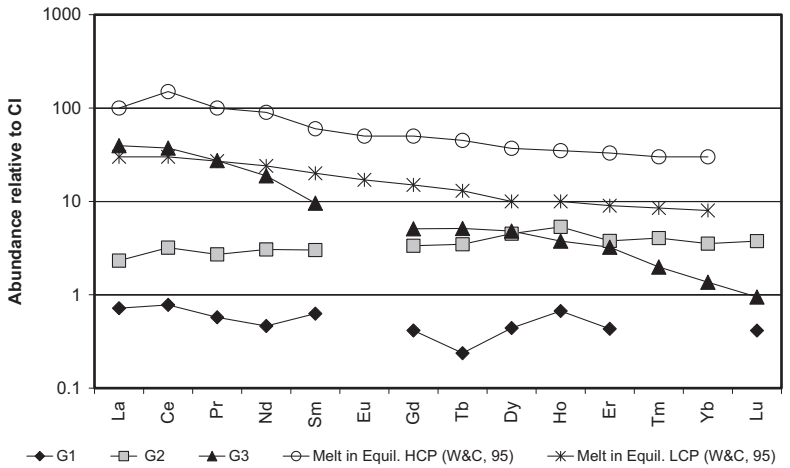
Abundance relative to CI
1000
100
10
1
0.1
La Ce Pr Nd Sm Eu Gd Tb Dy Ho Er Tm Yb Lu
G1
G2
G3
Melt in Equil. HCP (W&C, 95)
Melt in Equil. LCP (W&C, 95)

Fig. 8. A) Trace element distribution coefficients between the olivine host and the glass of the Chassigny GI G3 (Kd Ol/G3). The experimental olivine-liquid distribution coefficients (Experimental D) from Green (1994), McKay and Weill (1977), and Kennedy et al. (1993) are plotted for comparison. B) Trace element abundances of glasses G1 and G2 and the calculated liquids in equilibrium (L. Equil.) with low- and high-Ca pyroxenes (L. Equil. Px1, L. Equil. Px2, L. Equil. Cpx1, L. Equil. Cpx2, respectively). The low-Ca pyroxene-liquid distribution coefficients are for from Green (1994) and Kennedy et al. (1993); those for high-Ca pyroxene-liquid from Zajacz and Halter (2007). C) The CI-normalized REE abundances of the glasses G1, G2, and G3 in Chassigny are compared to the calculated melt in equilibrium with the early low-calcium pyroxene (LCP) (melt in equil. LCP) and late high-calcium pyroxene (HCP) phases (melt in equil. HCP) from Wadhwa and Crozaz (1995).

major element composition (Table 2). However, its unfractionated trace element pattern (La/Lu: 0.7) with abundances around 3 × CI clearly differs from those of maskelynite in others SNC meteorites (e.g., maskelynite in Shergotty, Wadhwa and Crozaz 1995). This is an evidence that G2 is not related to a plagioclase precursor. If it were the case, then it would be necessary to find a process that can explain the presence of two residual melts characterized by having different major and trace element compositions coexisting inside a single multiphase inclusion. We have not found such a process yet among closed-system processes.

The LREE-enrichment in the glassy inclusion G3 matches the La, Ce, Pr, and Nd abundances of the calculated melt in equilibrium with the early phases in Chassigny (Fig. 8C), but has lower abundances in Sm, Gd, Tb, Dy, Ho, Er, Tm, and Yb. The glassy inclusion G3 can be considered a possible infiltration that has been trapped by the olivine. However, if infiltration did occur, it must have been early in the crystallization sequence (Wadhwa and Crozaz 1995). Hence, we should expect the intercumulus melt to have achieved chemical equilibrium with the olivine. However, this is not the case.

In summary, the conditions prevailing during formation of these inclusions were such that equilibrium between phases inside inclusions, and between glasses and host minerals, could not been established. The compositional variability in glasses seems to be independent of the mineral phases making up the inclusion. Our data are therefore difficult to reconcile with the assumption that glass-bearing inclusions in Chassigny formed and evolved as a result of closed-system crystallization.

The Influence of Postformation Processes on Glass-Bearing Inclusions

Several lines of evidence show that secondary processes, such as impacts and/or fluid percolation, could have been strong enough to disturb ages in shergottites (Bouvier et al. 2009). The $^{40}Ar/^{39}Ar$ ages of maskelynite grains from ALHA 77005 suggest a complicated thermal history of this meteorite (Turrin et al. 2013). A recent study of several shocked shergottites gives ample evidence for pervasive shock-induced melting amounting to at least 23 vol% of these rocks. This event took place at pressures and temperatures close to 22 GPa and temperatures 1900 C < T < 2200 °C (Greshake and Fritz 2009; El Goresy et al. 2013). Heating experiments performed on glass inclusions of Chassigny indicate that temperatures of 1130–1150 °C are high enough to produce decrepitation of inclusions (Varela et al. 2000). Hence, we cannot discard the possibility that glass (or glass precursors) inside the inclusions could have been melted (totally or partially) and consequently could have flowed away and penetrated surrounding fractures. Indeed, the presence of glass in radial fractures was described for the Shergotty achondrite (El Goresy et al. 1997; Chen and El Goresy 2000). Therefore, we cannot rule out that part of the melt/fluid of the inclusions could have been lost, and consequently, their chemical compositions do not necessarily represent that of the original trapped melt.

Chassignites have also been affected by heating and deformation events whose nature and degree are still controversial (El Goresy et al. [2013] and reference therein). However, three features present in the glass-bearing inclusions (discussed in detail by Varela et al. [2000] and briefly mentioned below) suggest that this heating event must have been short.

First, all glass-bearing inclusions have high and variable contents of N, which is heterogeneously distributed in the glass.

Second, the radial fractures surrounding the inclusions have no traces of glass and the glass inside the inclusion is free of cracks (Fig. 1E). This suggests that the glass was soft during the event that fractured the minerals inside and around the inclusion. Therefore, the temperature must have been high enough for the glass to become soft but not high enough for it to become liquid. In this way the glass could not flow and thus could not fill cracks.

Third, glass inclusions that were heated in the laboratory (runs of ~8 h) are richer in K than those GIs that were not experimentally heated (Fig. 2B). This indicates a gain of K during the heating experiments, possibly from a nearby K source (the open radial cracks surrounding the inclusions?) where it had been deposited during the early heating event which caused

the cracking. The results of heating experiments indicate that K was mobilized during the postformational events that affected Chassigny. Such a disturbance (e.g., metasomatism?) could also trigger mobilization and redeposition of incompatible elements.

The compositional variability shown by the trace element contents of glasses, which cannot be explained by a closed-system igneous process, points in this direction. In addition, a recent SIMS study from the chassignite NWA 2737 shows that amphibole in melt inclusions lost ~0.6 wt% H_2O from an initial 0.7–0.8 wt% H_2O due to intense shock (Giesting et al. 2015). This is another indication that the initial composition of the glass-bearing inclusions has been modified.

Therefore, if the composition of the glass-bearing inclusions has been modified, it is not surprising that the experimental studies based on the parent magma composition determined by these inclusions were unable to produce the assemblage of phases observed in Chassigny (Minitti and Rutherford 2000; Filiberto et al. 2005).

High Abundance of Sr, Ba, Rb, B, and Be

Glass inclusions in Shergotty and Chassigny have high abundances in Sr, Ba, and Rb, as well as B and Be (Figs. 3 and 5). In Shergotty, the Rb and Sr abundances are higher in the GI trapped in a pigeonite core (826 and 236 ppm, respectively) than in the GIs trapped in the augite rim and titanomagnetite (303, 404 ppm [Rb]; 41.8 ppm [Sr]; Table 3) and glasses in merrillite have slightly lower Rb contents than GIs in pigeonite. Although the behavior of Sr is consistent with this element being compatible with plagioclase and apatite ($D > 1$, McKay et al. 1994; Prowatke and Klemme 2006), that of Rb appears to be in conflict with its incompatible nature ($D_{Rb\ (Plag\ and\ Apat)} < 1$, Bindeman et al. 1998; Prowatke and Klemme 2006). The Rb/Sr ratios in glasses of inclusions are highly variable in Chassigny. As mentioned above, primary inclusions hosted in the same olivine crystal show highly variable Rb/Sr ratios that are independent of inclusion type (e.g., glassy, monocrystalline, or multiphase inclusion). These inclusions show a slight positive K-Rb correlation (Varela et al. 2000).

The high abundances of incompatible elements in glasses of rhyolitic compositions appear to support the view of these glasses being residual melts. However, abundances and distributions of the REE in the very same glasses do not follow this view. Therefore, enrichment in incompatible elements (e.g., Be, Sr, Ba, and LREE) in glasses could be the result of some other process, like alteration involving fluids. Recently, McCubbin et al. (2013) suggested that the addition of a Cl-rich fluid during crystallization of the Chassigny intercumulus regions acted as both a chlorine source and a LREE source to the magma body. A modest enrichment of LREE is expected in Cl-rich fluids due to a slightly greater stability of aqueous LREE than that of HREE chloride complexes (Mayanovic et al. 2009). Although glasses in GI and MI in Chassigny are Cl-rich (~3000 ppm for GIs and MIs, Table 2), the observed compositional variation in both LREE and HREE appears much too large to be attributed only to the addition of a Cl-rich fluid. This is because immobile elements (e.g., high-field-strength elements [HFSE], REE) need very special conditions (such as high-K fluorine–rich melts) to be mobilized or redistributed (De Hoog and van Bergen 2000).

Therefore, we cannot exclude that some additional process, such as partial melting of phases inside inclusions during shock-induced melting, contributed to the enrichment of incompatible element (e.g., Be, Sr, Ba, and LREE).

In terrestrial rocks, a large range of concentrations of strongly incompatible elements such as Ba, Rb, Th, U, Ta, Nb, K, and La is a common feature of inclusions from different tectonic settings (e.g., midocean ridges and back-arc basin; Danyushevsky et al. 2004). The range in strongly incompatible element contents within a single sample or grain can exceed by more than one order of magnitude the range recorded by the host lavas (e.g., Sobolev and Shimizu 1993; Shimizu 1998; Danyushevsky et al. 2003). This compositional variability has been interpreted to originate by different processes, among them assimilation of wall-rock material in the magmatic plumbing system (e.g., Kent et al. 2002) or grain-scale reaction processes (Bedard et al. 2000) in which a dissolution–reaction–mixing process is involved (Danyushevsky et al. 2004). The latter can create large localized heterogeneity in major and trace element compositions, but do not necessary lead to obvious isotopic anomalies. However, as Mars, as far as we know, lacks the range of tectonic processes exhibited by Earth, comparison of the studied glass-bearing inclusion with those generates in magmatic plumbing systems should be taken with care.

CONCLUSIONS

Glasses from glass-bearing inclusions in Shergotty and Chassigny have similar major element compositions. All glasses are Si-rich with variable contents of Na_2O and K_2O that are negatively correlated with the SiO_2 content. They differ, however, in their Cl contents.

The chemical compositions of GIs in Shergotty reveal an unusual geochemistry in which glasses of GIs are out of equilibrium with their host crystals with trace

element contents that appear to be independent of their major element contents. The variability in the REE and light lithophile element contents of glasses is pronounced with LREE abundances that can vary by up to two orders of magnitude among different inclusions. The late-stage liquid (residual melts trapped by GIs in rims and late phases) is extremely depleted in REE.

In Chassigny, all types of inclusions record inhomogeneities and chemical variability in their major element contents (e.g., Na, K, Rb). The compositional heterogeneity in the REE content of glasses appears to be independent not only of the inclusions' types (GI or MI) but of the mineral phases making up the inclusion. Their chemical variability suggests formation and subsequent evolution of glass inclusions were such that equilibrium between phases inside inclusions and between glasses and host minerals could not be established.

The enrichment in incompatible elements (e.g., Be, Sr, Ba, and LREE) in glasses of glass-bearing inclusions in Shergotty and Chassigny signal some action of fluids and give additional evidence of their later transformation.

Our data are difficult to reconcile with the assumption that glass-bearing inclusions in Chassigny and Shergotty formed and evolved as a result of closed-system crystallization. The data show that the chemical composition of the glass-bearing inclusions was altered (as was the rock itself) by postformational processes whose nature we do not yet know in detail.

Our conclusions have direct implications on the effectiveness of these inclusions to remain as closed systems, shielded by their host crystals, and severely restrict their value as pristine samples.

We do not know whether these conclusions can be extended to other glass-bearing inclusions similarly surrounded by radial fractures in other SNC meteorites. Only more detailed studies of the individual constituents of these inclusions can give us the correct answer.

Acknowledgments—We are grateful to J. Gross, C. Goodrich, M. McCanta, and M. Jercinovic for constructive comments on a previous version of this manuscript. We thank Fanz Brandstätter (Naturhistorisches Museum Vienna) for supplying us with Shergotty and Chassigny thin sections. Financial support was received from CONICET (PIP 063) and Agencia (PICT 0142) Argentina.

Editorial Handling—Dr. Cyrena Goodrich

REFERENCES

Basu Sarbadhikari A., Goodrich C. A., Liu Y., Day J. M. D., and Taylor L. A. 2011. Evidence for heterogeneous enriched shergottite mantle sources in Mars from olivine-hosted melt inclusions in Larkman Nunatak 06319. *Geochimica et Cosmochimica Acta* 75:6803–6820.

Beck P., Barrat J.-A., Chaussidon M., Gillet P., and Bohn M. 2004. Li isotopic variations in single pyroxenes from the Northwest Africa 480 shergottite (NWA 480): A record of degassing of Martian magmas? *Geochimica et Cosmochimica Acta* 68:2925–2933.

Beck P., Barrat J. A., Gillet P., Wadhwa M., Franchi I. A., Greenwood R. C., Bohn M., Cotten J., de Moortele B. V., and Reynard B. 2006. Petrography and geochemistry of the chassignite Northwest Africa 2737 (NWA 2737). *Geochimica et Cosmochimica Acta* 70:2127–2139.

Bedard J. H., Hebert R., Berclaz A., and Varfalvy V. 2000. Syntexis and the genesis of lower oceanic crust. *Geological Society of America, Special Papers* 349:105–119.

Bindeman I. N., Davis A. M., and Drake M. J. 1998. Ion microprobe study of plagioclase-basalt partition experiments at natural concentration level of trace elements. *Geochimica et Cosmochimica Acta* 62:1175–1193.

Bouvier A., Blichert-Toft J., and Albarede F. 2009. Martian meteorite chronology and the evolution of the interior of Mars. *Earth and Planetary Science Letters*. 208:285–295.

Chen M. and El Goresy A. 2000. The nature of maskelynite in shocked meteorites: Not diaplectic glass but a glass quenched from shock-induced dense melt at high pressures. *Earth and Planetary Science Letters* 179:489–502.

Dann J. C., Holzheid A. H., Grove T. L., and Mc Sween H. Y. Jr. 2001. Phase equilibria of the Shergotty meteorite: Constraints on pre-eruptive water contents of Martian magmas and fractional crystallization under hydrous conditions. *Meteoritics & Planetary Science* 36:793–806.

Danyushevsky L. V., Della-Pasqua F. N., and Sokolov S. 2000. Reequilibration of melt inclusions trapped by magnesian olivine phenocrysts from subduction-related magmas: Petrological implications. *Contribution to. Mineralogy and Petrology* 138:68–83.

Danyushevsky L. V., McNeill A. W., and Sobolev A. V. 2002. Experimental and petrological studies of melt inclusions in phenocrysts from mantle-derived magmas: An overview of techniques, advantages and complications. *Chemical Geology* 183:5–24.

Danyushevsky L. V., Perfit M. R., Eggins S. M., and Falloon T. J. 2003. Crustal origin for coupled "ultra-depleted" and "plagioclase" signatures in MORB olivine-hosted melt inclusions: Evidence from the Siqueiros Transform Fault, East Pacific Rise. *Contributions to Mineralogy and Petrology* 144:619–637.

Danyushevsky L. V., Leslie R. A. J., Crawford A. J., and Durance P. 2004. Melt inclusions in primitive olivine phenocrysts: The role of localized reaction processes in the origin of anomalous compositions. *Journal of Petrology* 45:2531–2553.

De Hoog J. C. M. and van Bergen J. 2000. Volatile-induced transport of HFSE, REE, Th and U in arc magmas: Evidence from zirconolite-bearing vesicles in potassic lavas of Lenwotolo volcano (Indonesia). *Contribution to Mineralogy and Petrology* 139:485–502.

El Goresy A., Wopenka B., Chen M., and Kurat G. 1997. The saga of Maskelynite in Shergotty. *Meteoritics & Planetary Science* 32:A38–A39.

El Goresy A., Gillet P., Miyahara M., Ohtani E., Ozawa S., Beck P., and Montagnac G. 2013. Shock-induced deformation of Shergottites: Shock-pressures and

perturbations of magmatic ages on Mars. *Geochimica et Cosmochimica Acta* 101:233–262.
Faure F. and Schiano P. 2005. Experimental investigation of equilibration conditions during forsterite growth and melt inclusion formation. *Earth and Planetary Science Letters* 236:882–898.
Filiberto J. 2008. Experimental constraints on the parental liquid of the Chassigny meteorite: A possible link between the Chassigny meteorite and a Martian Gusev basalt. *Geochimica et Cosmochimica Acta* 72:690–701.
Filiberto J., Nekvasil H., and Lindsley D. H. 2005. An experimental crystallization study of a proposed high-Fe, low-Al Martian parental liquid at elevated pressure (abstract #1359). 36th Lunar and Planetary Science Conference. CD-ROM.
Floran R. J., Prinz M., Hlava P. F., Keil K., Nehru C. E., and Hinthorne J. R. 1978. The Chassigny meteorite: A cumulate dunite with hydrous amphibole-bearing melt inclusions. *Geochimica et Cosmochimica Acta* 42:1213–1229.
Gaetani G. A. and Watson E. B. 2000. Open system behavior of olivine-hosted melt inclusions. *Earth and Planetary Science Letters* 183:27–41.
Giesting P. A., Schwenzer S. P., Filiberto J., Starkey N. A., Franchi I. A., Treiman A. H., Tindle A., and Grady M. M. 2015. Igneous and shock processes affecting chassignite amphibole evaluated using chlorine/water partitioning and hydrogen isotopes. *Meteoritics and Planetary Science* 50:433–460.
Giletti B. J. and Shanahan T. M. 1997. Alkali diffusion in plagioclase feldspar. *Chemical Geology* 139:3–20.
Goodrich C. A. 2002. Olivine-phyric Martian basalts: A new type of shergottite. *Meteoritics and Planetary Science* 37: B31–B34.
Goodrich C. A. 2003. Petrogenesis of olivine-phyric shergottites Sayh al Uhaymir 005 and Elephant Moraine A79001 lithology A. *Geochimica et Cosmochimica Acta* 67:3735–3771.
Goodrich C. A., Treiman A. H., Filiberto J., Gross J., and Jercinovic M. 2013. K_2O-rich trapped melt in olivine in the Nakhla meteorite: Implications for petrogenesis of nakhlites and evolution of the Matian mantle. *Meteoritics & Planetary Science* 48:2371–2405.
Green T. H. 1994. Experimental studies of trace-element partitioning applicable to igneous petrogenesis—Sedona 16 years later. *Chemical Geology* 117:1–36.
Greshake A. and Fritz J. 2009. Discovery of ringwoodite, wadsleyite, and ?-$Ca_3(PO_4)_2$ in Chassigny: Constraints on shock conditions (abstract #1586). 40th Lunar and Planetary Science Conference. CD-ROM.
Harvey R. P. and McSween H. Y. Jr. 1992. Parent magma of the nakhlite meteorites: Clues from melt inclusions. *Earth and Planetary Science Letters* 111:467–482.
Herd C. D. K., Treiman A. H., McKay G. A., and Shearer C. K. 2004. The behavior of Li and B during planetary basalt crystallization. *American Mineralogist* 89:832–840.
Herd C. D. K., Treiman A. H., McKay G. A., and Shearer C. K. 2005. Light lithophile elements in Martian basalts: Evaluating the evidence for magmatic water degassing. *Geochimica et Cosmochimica Acta* 69:2431–2440.
Hewins R. H., Zanda B., Pont S., Humayun M., Assayag N., and Cartigny P. 2015. Northwest Africa 8694, a ferroan chassignite (abstract # 2249). 46th Lunar and Planetary Science Conference. CD-ROM.
Johnson M. C., Rutherford M. J., and Hess P. C. 1991. Chassigny petrogenesis: Melt compositions, intensive parameters, and water contents of Martian (?) magmas. *Geochimica et Cosmochimica Acta* 55:349–366.
Kennedy A. K., Lofgren G. E., and Wassenburg G. J. 1993. An experimental study of trace element partitioning between olivine, orthopyroxene and melt in chondrules: Equilibrium values and kinetic effects. *Earth and Planetary Science Letters* 115:177–195.
Kent A. J. R., Baker J. A., and Wiedenbeck M. 2002. Contamination and melt aggregation processes in continental flood basalts: Constraints from melt inclusions in Oligocene basalts from Yemen. *Earth and Planetary Science Letters* 202:577–594.
Lentz R. C. F., McSween H. Y., Ryan J., and Riciputi L. R. 2001. Water in Martian magmas: Clues from light lithophile elements in shergottite and nakhlite pyroxenes. *Geochimica et Cosmochimica Acta* 65:4551–4565.
Lodders K. 2003. Solar system abundances and condensation temperatures of the elements. *Astrophysical Journal* 591:1220–1247.
Lodders K. and Fegley B. 1998. *The planetary scientist's companion*. New York: Oxford University Press.
Lundberg L. L., Crozaz G., McKay G., and Zinner E. 1988. Rare earth element carriers in the Shergotty meteorite and implications for its chronology. *Geochimica et Cosmochimica Acta* 52:2147–2163.
Mayanovic R. A., Anderson A. J., Bassett W. A., and Chou I. M. 2009. The structure and stability of aqueous rare-earth elements in hydrothermal fluids: New results on neodymium(III) aqua and chloroaqua complexes in aqueous solutions to 500 degrees C and 520 MPa. *Chemical Geology* 259:30–38.
McCanta M. C., Elkins-Tanton L., and Rutherford M. J. 2009. Expanding the application of the Eu-oxybarometer to the lherzolitic shergottites and nakhlites: Implications for the oxidation state heterogeneity of the Martian interior. *Meteoritics & Planetary Science* 44:725–745.
McCubbin F. M. and Nekvasil H. 2008. Maskelynite-hosted apatite in the Chassigny meteorite: Insights into late-stage magmatic volatile evolution in Martian magmas. *American Mineralogist* 93:676–684.
McCubbin F. M., Nekvasil H., Harrington A., Elardo S., and Lindsley D. H. 2007. Experimental crystallization of dry and wet Humphrey at 9.3 kbar: Implications for compositional diversity of the Martian crust. American Geophysical Union #P13E-07.
McCubbin F. M., Elardo S. M., Shearer J. R. C. K., Smirnov A., Hauri E. H., and Draper D. S. 2013. A petrogenetic model for the comagmatic origin of chassignites and nakhlites: Inferences from chlorine-rich minerals, petrology, and geochemistry. *Meteoritics & Planetary Science* 48:819–853.
McKay G. A. and Weill D. F. 1977. KREEP petrogenesis revisited. Proceedings, 8th Lunar Science Conference. pp. 2339–2355.
McKay G. A., Le L., Wagstaff J., and Crozaz G. 1994. Experimental partitioning of rare earth elements and strontium: Constraints on petrogenesis and redox conditions during crystallization of Antarctic angrite Lewis Cliff 86010. *Geochimica et Cosmochimica Acta* 58:2911–2919.
McSween H. Y. 1985. SNC meteorites: Clues to Martian petrologic evolution? *Reviews of Geophysics* 23:391–416.

McSween H. Y. 1994. What we have learned about Mars from SNC meteorites. *Meteoritics* 29:757–779.

McSween H. Y. and Treiman A. H. 1998. Martian meteorites. In *Planetary materials*, edited by Papike J. J. Washington, D.C.: Mineralogical Society of America. pp. F1–F53.

McSween H. Y., Grove T. L., Lentz R. C. F., Dann J. C., Holzheid A. H., Riciputi L. R., and Ryan J. G. 2001. Geochemical evidence for magmatic water within Mars from pyroxenes in the Shergotty meteorite. *Nature* 409:487–490.

Minitti M. E. and Rutherford M. J. 2000. Genesis of the Mars Pathfinder "sulfur-free" rock from SNC parental liquids. *Geochimica et Cosmochimica Acta* 64:2535–2547.

Mittlefehldt D. W. 1994. ALH 84001, a cumulate orthopyroxenite member of the Martian meteorite clan. *Meteoritics* 29:214–221.

Mosbah M., Metrich N., and Massiot P. 1991. PIGME fluorine determination using a nuclear microprobe with applications to glass inclusions. *Nuclear Instruments and Methods B* 58:227–231.

Nekvasil H., Filiberto J., McCubbin F. M., and Lindsley D. H. 2007. Alkalic parental magmas for the chassignites? *Meteoritics & Planetary Science* 42:979–992.

Peslier A. H., Hnatyshin D., Herd C. D. K., Walton E. L., Brandon A. D., Lapen T. J., and Shafer J. T. 2010. Crystallization, melt inclusion, and redox history of a Martian meteorite: Olivine-phyric shergottite Larkman Nunatak 06319. *Geochimica et Cosmochimica Acta* 74:4543–4576.

Prowatke S. and Klemme S. 2006. Trace element partitioning between apatite and silicate melts. *Geochimica et Cosmochimica Acta* 70:4513–4527.

Richter F. M., Chaussidon M., and Watson E. B. 2013. Lithium isotope fractionation by diffusion of augites in laboratory experiments and in Martian meteorite MIL 03346 (abstract #1526). 44th Lunar and Planetary Science Conference. CD-ROM.

Roedder E. 1984. Fluid inclusions. *Review in Mineralogy* 12:644.

Sautter V., Toplis M. J., Lorand J. P., and Macri M. 2012. Melt inclusions in augite from the nakhlite meteorites: A reassessment of nakhlite parental melt and implications for petrogenesis. *Meteoritics & Planetary Science* 47:330–344.

Shimizu N. 1998. The geochemistry of olivine-hosted melt inclusions in a FAMOUS basalt ALV519-4-1. *Physics of the Earth and Planetary Interiors* 107:183–201.

Sobolev A. V. 1996. Melt inclusions in minerals as a source of principle petrological information. *Petrology* 4: 209–220.

Sobolev A. V. and Shimizu N. 1993a. Ultra-depleted primary melt included in an olivine from the Mid-Atlantic Ridge. *Nature* 363:151–154.

Sonzogni Y. and Treiman A. H. 2013. Small melt inclusions in olivines from Martian meteorites. Value for constraining original melt composition (abstract #1049). 44th Lunar and Planetary Science Conference. CD-ROM.

Stockstill K. R., Bodnar R. J., and McSween H. Y. 2005. Melt inclusions in augite of the Nakhla Martian meteorite: Evidence for basaltic parental melt. *Meteoritics & Planetary Science* 40:377–396.

Stolper E. and McSween H. Y. Jr. 1979. Petrology and origin of the shergottite meteorites. *Geochimica et Cosmochimica Acta* 43:1475–1498.

Treiman A. H. 1986. The parental magma of the Nakhla achondrite: Ultrabasic volcanism on the shergottite parent body. *Geochimica et Cosmochimica Acta* 50:1061–1070.

Treiman A. H. 1993. The parent magma of the Nakhla (SNC) meteorite, inferred from magmatic inclusions. *Geochimica et Cosmochimica Acta* 57:4753–4767.

Treiman A. H. 2005. The nakhlite meteorites: Augite-rich igneous rocks from Mars. *Chemie der Erde-Geochemistry* 65:203–270.

Treiman A. H., McKay G. A., Bogard D. D., Wang M. S., Lipschultz M. E., Mittlefehldt D. W., Keller L., Lindstrom M. M., and Garrison D. 1994. Comparison of the LEW 88516 and ALHA77005 Martian meteorites: Similar but distinct. *Meteoritics* 29:581–592.

Treiman A. H., Musselwhite D. S., Herd C. D. K., and Shearer C. K. Jr. 2006. Light lithophile elements in pyroxenes of Northwest Africa (NWA) 817 and other Martian meteorites: Implications for water in Martian magmas. *Geochimica et Cosmochimica Acta* 70:2919–2934.

Turrin B., Park J., Herzog G. F., Lindsay F. N., Delaney J. S., Nyquist L. E., and Swisher C. C. 2013. $^{40}Ar/^{39}Ar$ ages of maskelynite grains from ALHA 77005 (abstract #2979). 44th Lunar and Planetary Science Conference. CD-ROM.

Varela M. E. and Zinner E. 2013. Glass bearing inclusions in Shergotty (abstract #1501). 44th Lunar and Planetary Science Conference. CD-ROM.

Varela M. E., Kurat G., Bonnin-Mosbah M., Clocchiatti R., and Massare D. 2000. Glass-bearing inclusions in olivine of the Chassigny achondrite: Heterogeneous trapping at sub-igneous temperatures. *Meteoritics & Planetary Science* 35:39–52.

Varela M. E., Kurat G., and Clocchiatti R. 2001. Glass-bearing inclusions in Nakhla (SNC meteorite) augite: Heterogeneously trapped phases. *Mineralogy and Petrology* 71:155–172.

Varela M. E., Kurat G., and Clocchiatti R. 2003. Answer to Treiman's comment: The Nakhla meteorite is a cumulate igneous rock. *Mineralogy and Petrology* 77:279–285.

Wadhwa M. and Crozaz G. 1995. Trace and minor elements in minerals of nakhlites and Chassigny—Clues to their Petrogenesis. *Geochimica et Cosmochimica Acta* 59:3629–3645.

Wadhwa M., McSween H. Y., and Crozaz G. 1994. Petrogenesis of shergottite meteorites inferred from minor and trace element microdistributions. *Geochimica et Cosmochimica Acta* 58:4213–4229.

William C. D., Wadhwa M., Bell D. R., and Hervig R. 2010. Light lithophile element microdistribution in pyroxenes of the Martian meteorites (abstract #2641). 41st Lunar and Planetary Science Conference. CD-ROM.

Zajacz Z. and Halter W. 2007. LA-ICPMS analyses of silicate melt inclusions in co-precipitated minerals: Quantification, data analysis and mineral/melt partitioning. *Geochimica et Cosmochimica Acta* 71:1021–1040.

Zinner E. and Crozaz G. 1986. A method for the quantitative measurement of rare earth elements in the ion microprobe. *International Journal of Mass Spectrometry Ion Proceeding* 69:17–38.